

ESTIMATION OF WIDE BAND RADAR CROSS SECTION (RCS) OF REGULAR SHAPED OBJECTS USING METHOD OF MOMENTS (MOM)

M. Madheswaran¹ and P. Suresh Kumar²

Center for Advanced Research, Department of Electronics and Communication Engineering, Muthayammal Engineering College, India
E-mail: ¹madheswaran.dr@gmail.com and ²sureshk.eee@gmail.com

Abstract

Modern fighter aircrafts, ships, missiles etc need to be very low Radar Cross Section (RCS) designs, to avoid detection by hostile radars. Hence accurate prediction of RCS of complex objects like aircrafts is essential to meet this requirement. A simple and efficient numerical procedure for treating problems of wide band RCS prediction Perfect Electric Conductor (PEC) objects is developed using Method of Moment (MoM). Implementation of MoM for prediction of RCS involves solving Electric Field Integral Equation (EFIE) for electric current using the vector and scalar potential solutions, which satisfy the boundary condition that the tangential electric field at the boundary of the PEC body is zero. For numerical purposes, the objects are modeled using planar triangular surfaces patches. Set of special sub-domain type basis functions are defined on pairs of adjacent triangular patches. These basis functions yield a current representation free of line or point charges at sub-domain boundaries. Once the current distribution is obtained, dipole model is used to find Scattering field in free space. RCS can be calculated from the scattered and incident fields. Numerical results for a square plate, a cube, and a sphere are presented over a bandwidth.

Keywords:

Dipole Model, Method of Moment (MoM), Perfectly Electric Conductor (PEC), Radar Cross Section (RCS), Triangular Patch Model

1. INTRODUCTION

The estimation of RCS has been the field of focus in the recent years for various purposes. The accurate estimation has been taken by many researches using different techniques. The regular shaped objects at high frequencies impose a challenging task for the researchers to estimate RCS. E.F.Knott et al., [2] have reported the MoM for prediction of RCS by solving EFIE for electric current using the vector and scalar potential solutions. In arbitrary surface modeling the EFIE has the advantage of being applicable to both open and close bodies whereas the MFIE are applied only to closed surfaces. Johnson J.H.Wang [1] has detailed based on Galerkin's technique to solve simultaneous equations of MFIE. There are notable approaches that have been used to form integral equation for Method of Moments. The surface of the body is generally modeled either as a wire-mesh (wire-grid model) or a surface partitioned into smooth or piecewise smooth (surface patch model). Some of the problems encountered in wire grid model include the presence of fictitious loop currents in the solution, ill-conditioned moment matrices and incorrect currents at the cavity resonant frequencies of the scatterer. The difficulties in interpreting computed wire currents and relating them to equivalent surface currents [3].

J.H. Richmond [4] has discussed wire mesh model to predict the RCS of closed surface. It provided poor accuracy compared

to the theoretical values. K.S.H.Lee et al., [5] have proposed a method to predict the RCS of simple cube and metallic device using wire grid model. Prediction has done considering the patches as rectangular mesh. The measurement results indicate that the wire grid model have accurate for simple objects and difficult for complex objects. Most of these difficulties can be either wholly or partially overcome by surface patch approaches. An efficient computational technique for obtaining scattering cross sections of electrically small aircraft at low frequencies is presented by Yah T. Lin et al., [6]. It has based on the wire-grid reaction method works as an efficient target identification technique at low frequencies.

T.S.M. Rao et al., [7] have developed an efficient procedure for plane wave, circular and square objects using by combining EFIE and triangular surface patches. It overcomes the problems focused by wire grid methods. Virga, K.L. and Rahmat-Samii, Y [8] have presented a methodology to obtain monostatic radar cross section of a finite-size perfectly conducting flat plate using triangular patch mesh profile. The RCS obtained shows better results in low frequency region as compared to physical optics.

Two different numerical methods based on MoM and physical objects was proposed by Sidhu, J.S [9] to analyze the RCS of complex scattering objects in resonance frequency Region. Numerical results indicate that MoM provides high accuracy compared to physical objects in resonance frequency region. Do-Hoon Kwon et al., [10] have introduced a method to reduce the computer processing time to estimate the Monostatic RCS of simple objects using MoM based surface patch model. In that case, the unknown surface currents have expressed in terms of basis functions.

X. F. Li et al., [11] have presented an accurate and efficient approach to predict the bistatic RCS of electrically large PEC targets. A current matching technique was introduced into the conventional high-frequency method to obtain bistatic RCS. The high frequency surface wave radar has been numerically evaluated by combining finite-difference time-domain (FDTD) method and the MoM was presented in [12]. It has provided good results when the range of RCS is 5 to 60 dB.

2. MOM IMPLEMENTATION

The estimation of RCS of a PEC is determined by applying Method of Moments (MoM) using the Electric Field Integral Equation (EFIE). The MoM is an integral based algorithm. Consider an arbitrarily shaped perfect electric conductor shown in Fig.1. The PEC surface has divided into triangular sub-domains using surface patch model. The simultaneous equations have been generated over the sub-domains and added together to form a global matrix equation. The solution of the matrix gives electric current distribution in the surface of the PEC objects.

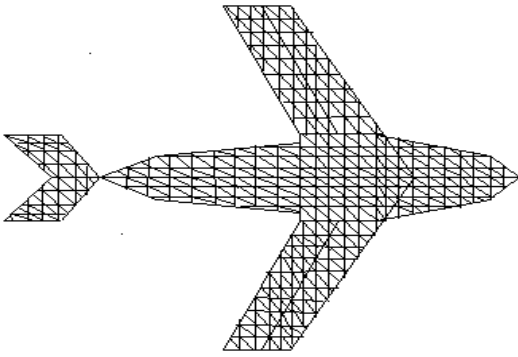


Fig.1. Aircraft surface modeled by triangular patches

Consider the inhomogeneous equations [6],

$$L(f) = g \tag{1}$$

where, L is a linear operator, g is known and f is to be determined. Let f be expanded in a series of functions $f_1, f_2, f_3 \dots$ as,

$$f = \sum_n \alpha_n f_n \tag{2}$$

where, α_n is a constant. The function f_n is called expansion functions or basis functions. For exact solutions, the above equation is an infinite summation and the form a complete set of basis functions. For approximate solutions, this has usually a finite summation.

From the above two equations,

$$\sum_n \alpha_n L(f_n) = g \tag{3}$$

Now define a set of weighting functions, or testing functions, $w_1, w_2, w_3 \dots$ in the range of L , and take the inner product of the above equation with each w_n . The result is,

$$\sum_n \alpha_n \langle w_n, Lf_n \rangle = \langle w_n, g \rangle \quad m = 1, 2, 3, \dots \tag{4}$$

This set of equation can be written in matrix form as,

$$[l_{mn}] [\alpha_n] = [g] \tag{5}$$

where,

$$[l_{mn}] = \begin{bmatrix} \langle w_1, Lf_1 \rangle & \langle w_1, Lf_2 \rangle & \dots \\ \langle w_2, Lf_1 \rangle & \langle w_2, Lf_2 \rangle & \dots \\ \dots & \dots & \dots \end{bmatrix} \tag{6a}$$

$$[\alpha_n] = \begin{bmatrix} \alpha_1 \\ \alpha_2 \\ \vdots \\ \vdots \end{bmatrix} \quad [g_m] = \begin{bmatrix} \langle w_1, g \rangle \\ \langle w_2, g \rangle \\ \vdots \\ \vdots \end{bmatrix} \tag{6b}$$

If the matrix $[l]$ is nonsingular its inverse $[l^{-1}]$ exists. α_n can also be represented as,

$$[\alpha_n] = [l_{mn}^{-1}] [g_m] \tag{7}$$

and the solution for f is given by, $f = \sum_n \alpha_n f_n$. For concise expression of this result, define the matrix of functions

$$[\tilde{f}_n] = [f_1, f_2, \dots] \tag{8}$$

and the value of \hat{f} is given as,

$$\hat{f} = [\tilde{f}_n] [\alpha_n] = [\tilde{f}_n] [l_{mn}^{-1}] [g_m] \tag{9}$$

This solution may be exact or approximate, depending upon the choice of the f_n and w_n . The particular choice $f_n = w_n$ is known as Galerkin's method.

2.1 ELECTRIC FIELD INTEGRAL EQUATION (EFIE)

Let S denotes the surface of an open or closed perfectly conducting object with unit normal \hat{n} . An electric field, defined to be the field due to an impressed source in the absence of the object, is incident on and induces surface currents J on S .

The scattering electric field E^s can be computed from the surface current by [7]

$$E^s = -j\omega A - \nabla\Phi \tag{10}$$

with the magnetic vector potential defined as,

$$A(r) = \frac{\mu}{4\pi} \int_S \frac{J e^{-jkR}}{R} dS' \tag{11}$$

and the electric scalar potential as,

$$\Phi(r) = \frac{1}{4\pi\epsilon} \int_S \frac{\sigma e^{-jkR}}{R} dS' \tag{12}$$

where, k is wave number and $R = |r - r'|$ is the distance between an arbitrarily located observation point r and a source point r' on S . Both r and r' are defined with respect to a global coordinate origin O . The surface charge density σ is related to surface divergence of J through the equation of continuity,

$$\nabla_s \cdot J = -j\omega\sigma \tag{13}$$

We derive an integro-differential equation for J by enforcing the boundary condition,

$$\hat{n} \times (E^s + E^i) = 0 \quad \text{on } S, \text{ obtaining} \tag{14}$$

$$\hat{n} \times E^s = -\hat{n} \times E^i = \hat{n} \times (-j\omega A - \nabla\Phi), \quad r \text{ on } S \tag{15}$$

$$-E_{\tan}^i = (-j\omega A - \nabla\Phi)_{\tan}, \quad r \text{ on } S \tag{16}$$

the above equation is the so-called electric field equation [8].

2.2 BASIS FUNCTION FORMULATION

The basis function defined on a pair of triangular patches and sharing a common (interior) edge as shown in the Fig.2 and Fig.3.

Points in T_n^+ triangle may be designated either by the position vector r defined with respect to O , or by free position vector ρ_n^+ defined with respect to and away from the free vertex of T_n^+ . For points in triangle T_n^- may be designated either by the position vector r defined with respect to O , or by free position vector ρ_n^- defined with respect to and toward the free vertex of T_n^- . This designation is chosen so that a positive current vector associated with edge l_n is from triangle T_n^+ to triangle T_n^- . The surface

divergence of \mathbf{f}_n in T_n^\pm , which is proportional to the surface charge density associated with the basis element, is,

$$\nabla \cdot \mathbf{f}_n = \begin{cases} \frac{l_n}{A_n^+}, & \mathbf{r} \text{ in } T_n^+ \\ -\frac{l_n}{A_n^-}, & \mathbf{r} \text{ in } T_n^- \\ 0, & \text{otherwise} \end{cases} \quad (22)$$

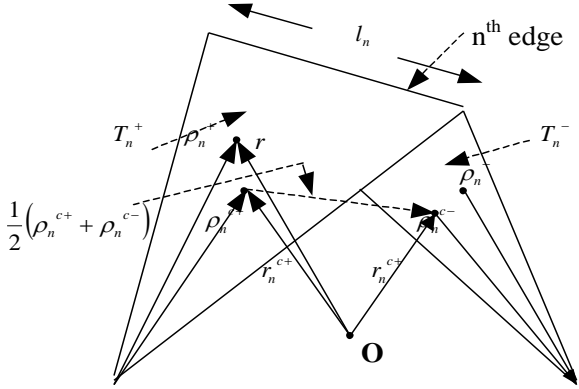


Fig.2. Triangle pair and geometrical parameter associated with interior edge

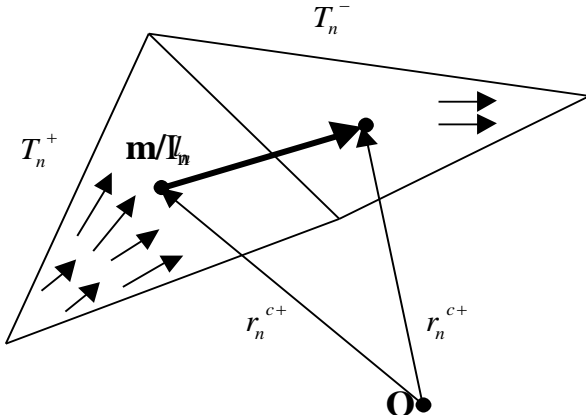


Fig.3. Dipole model of an edge element

Since the surface divergence in T_n^\pm is $(\pm 1/\rho_n^\pm) \partial(\rho_n^\pm f_n)/\partial\rho_n^\pm$. The charge density is thus constant in each triangle. The current on \mathbf{S} may be approximated in terms of the \mathbf{f}_n as,

$$\mathbf{J} \cong \sum_{n=1}^N I_n \mathbf{f}_n(\mathbf{r}) \quad (23)$$

where, N is the number of interior (non-boundary) edges. Since a basis function is associated with each non-boundary edge, each triangle patch has up to three basis functions of currents flowing on it.

Substituting the current expression in a $N \times N$ system of linear equations, the impedance matrix can be formulated as,

$$\mathbf{Z} = \mathbf{I}\mathbf{V}$$

where, $\mathbf{Z} = [Z_{mn}]$ is an $N \times N$ matrix and $\mathbf{I} = [I_n]$ and $\mathbf{V} = [V_m]$ are column vectors of length N . Elements of \mathbf{Z} and \mathbf{V} are given by,

$$Z_{mn} = l_m \left[j\omega \left(\mathbf{A}_{mn}^+ \cdot \frac{\rho_m^+}{2} + \mathbf{A}_{mn}^- \cdot \frac{\rho_m^-}{2} \right) + [\Phi_{mn}^+ - \Phi_{mn}^-] \right] \quad (24)$$

$$V_m = l_m \left(\mathbf{E}_m^+ \cdot \frac{\rho_m^{c+}}{2} + \mathbf{E}_m^- \cdot \frac{\rho_m^{c-}}{2} \right) \quad (25)$$

where,

$$\mathbf{A}_{mn}^\pm = \int_s \mathbf{f}_n(\mathbf{r}') \frac{e^{-jkR_m^\pm}}{R_m^\pm} d\mathbf{S}' \quad (26)$$

$$\Phi_{mn}^\pm = -\frac{1}{4\pi j\omega\epsilon_s} \int_s \nabla'_s \cdot \mathbf{f}_n(\mathbf{r}') \frac{e^{-jkR_m^\pm}}{R_m^\pm} d\mathbf{S}' \quad (27)$$

$$\mathbf{R}_m^\pm = |\mathbf{r}_m^{c\pm} - \mathbf{r}'| \text{ and} \quad (28)$$

$$\mathbf{E}_m^\pm = \mathbf{E}^i \mathbf{r}_m^{c\pm} \quad (29)$$

These equations provide elements of the moment matrix and the forcing vector \mathbf{V} .

2.3 DIPOLE MODEL

Once surface currents are known on the object surface, a radiated electromagnetic signal in free space can be calculated by a number of approaches. One method is dipole model [15]. In dipole model the surface current distribution for each edge element containing two triangles is replaced by an infinitesimal dipole, having an equivalent dipole moment or strength. The basis function defined on a pair of triangular patches and sharing a common (interior) edge as shown in the Fig.3. The radiated field of a small dipole is the well-known analytical expression. The total radiated field is then obtained as a sum of the contributions of infinitesimal dipoles.

To find the equivalent dipole moment, consider an edge element m which is the product of an effective dipole current and effective dipole length is obtained by the integration of the surface current, corresponding to edge element m , over the element surface:

$$\begin{aligned} \mathbf{m} &= \int_{T_m^+ + T_m^-} I_m \mathbf{f}_m(\mathbf{r}) d\mathbf{S} = \int_{T_m^+ + T_m^-} \mathbf{f}_m(\mathbf{r}) d\mathbf{S} \\ &= l_m I_m (\mathbf{r}_m^{c+} + \mathbf{r}_m^{c-}) \end{aligned} \quad (30)$$

Here, $\mathbf{f}_m(\mathbf{r})$ is the edge element basis function.

The radiated magnetic and electric fields of an infinitesimal dipole located at the origin is expressed at a point \mathbf{r} in terms of vector notations as,

$$\mathbf{H}(\mathbf{r}) = \frac{jk}{4\pi} (\mathbf{m} \times \mathbf{r}) C e^{-jkr}, \quad C = \frac{1}{r^2} \left[1 + \frac{1}{jkr} \right] \quad (31)$$

$$\mathbf{E}(\mathbf{r}) = \frac{\eta}{4\pi} \left((\mathbf{M} - \mathbf{m}) \left[\frac{jk}{r} + C \right] + 2\mathbf{M}\mathbf{C} \right) e^{-jkr}$$

where,

$$\mathbf{M} = \frac{(\mathbf{r} \cdot \mathbf{m})\mathbf{r}}{r^2}, r = |\mathbf{r}|,$$

$\eta = \sqrt{\mu/\epsilon} = 377\Omega$ is the free space impedance.

The total electric and magnetic field at a point \mathbf{r} are obtained as a sum over all edge elements.

$$\mathbf{E}(\mathbf{r}) = \sum_{m=1}^M \mathbf{E}_m - \frac{1}{2}(\mathbf{r}_m^{c+} + \mathbf{r}_m^{c-}) \tag{32}$$

$$\mathbf{H}(\mathbf{r}) = \sum_{m=1}^M \mathbf{H}_m - \frac{1}{2}(\mathbf{r}_m^{c+} + \mathbf{r}_m^{c-}) \tag{33}$$

From the incident electric and the estimated electric fields, the Radar Cross Section can be calculated as [2]

$$\sigma = 4\pi R^2 \frac{|\mathbf{E}^s|^2}{|\mathbf{E}^i|^2} \tag{34}$$

3. RESULTS

To validate the analysis presented in the previous sections, a few numerical examples are considered. The first geometry considered is a dielectric sphere of radius $r = 0.2\lambda$ with the incident electric field at 0 degrees and $\alpha = 90$ degrees. The frequency responses from 2GHz to 8GHz are plotted in Fig.4. The sphere is discretized with 500 triangular elements resulting into 706 unknown current coefficients. It can be observed that the EFIE along it produces more accurate for the whole frequency band and angular domains. For 706 unknowns, exact solution took around 260 seconds CPU time to fill the matrix.

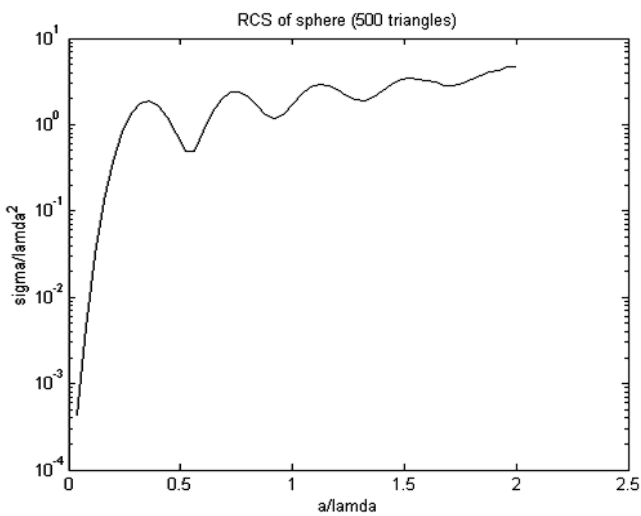


Fig.4. RCS of a sphere

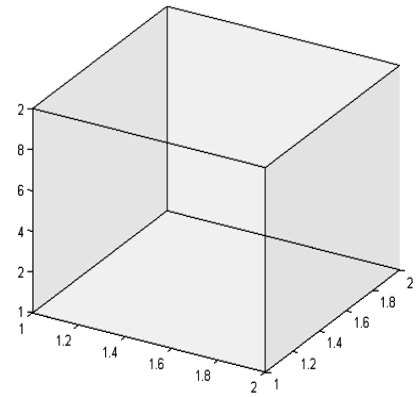


Fig.5. Cube with dimensions (2 x 2 x 2)

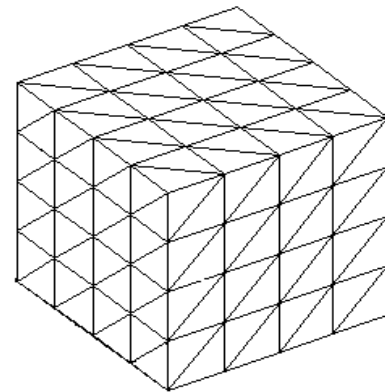


Fig.6. Mesh structure in 3D cube

The monostatic RCS frequency and angular response of a PEC cube (2cm x 2cm x 2cm) is calculated by MoM integral equations based on dipole model with $\varphi = 0$. The cube is discretized with 850 triangular elements resulting into 1226 unknown current coefficients. Fig.7 shows the frequency response of a cube is plotted at various frequencies and compared with Finite Element Method. It shows that the result of proposed method is more agreed with theoretical measurements.

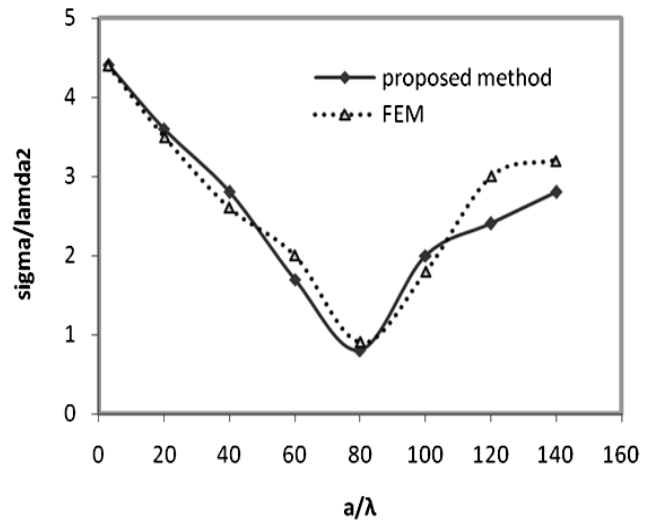


Fig.7. Monostatic RCS of a cube at $\varphi = 0$

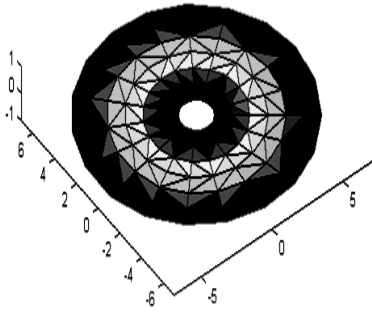


Fig.8. Mesh structure in 3D cylinder

The monostatic RCS of a cylinder shown in Fig.8 is calculated, where, $a = 0.15\text{m}$, $h = 0.5\text{m}$, and $l = 0.8\text{m}$. The frequency of the incident planar wave which is horizontal polarized is 3GHz. The comparison between the monostatic RCS calculated by the expression and MoM are compared. It shows that the proposed method is good agreement with theoretical results.

Table.1 shows the cube with various dimensions and frequencies. It is observed that an increase in the dimension of a cube results in different RCS values. The frequencies of a cube also make an increase in the RCS estimation.

Table.1. RCS of Cube at various dimensions and frequencies

Size of the Cube(cm)	σ/λ^2 at various frequencies in GHz		
	2 GHz	2.35GHz	2.5GHz
2	0.42	0.58	0.67
3	0.58	0.63	0.76
4	0.82	0.89	0.98
5	1.23	1.45	1.87
6	1.65	1.89	2.56

Table.2 shows the computation time required for a sphere in various dimensions. The incident angle and the triangular elements are taken as constant values. It is observed that the dimension of a sphere is increased; the triangle size gets increased and needs more matrix elements for computation which in turn increases the computation time.

Table.2. Size of sphere vs computation time

Object (Sphere) Radius (cm)	Incident Angle (θ) degrees	No of triangular elements	Computation Time(sec)
1	0	500	260
1.5	0	502	302
2	0	502	346
2.5	0	502	408
3	0	502	460

Table.3 shows the radar cross section of a cylinder at $r = 1\text{cm}$ and $h = 1\text{cm}$ with the frequency 9GHz. The RCS was estimated using FEM, Method of Moments. The estimated values are also compared with the theoretical value. It was observed that the RCS estimation based on Method of Moments provides an accurate value compared to FEM.

Table.3. Radar cross section of a cylinder at $r = 1\text{cm}$ and $h = 1\text{cm}$ and frequency $f = 9\text{GHz}$

Aspect angle in degrees	Radar cross section (dB) of a cylinder at $r = 1\text{cm}$ and $h = 1\text{cm}$, $f = 9\text{GHz}$		
	Theoretical	FEM	MOM
0	-50	-44	-46
20	-43	-37.3	-36.6
40	-38.8	-32	-33.1
60	-33.7	-25.1	-24
80	-23.9	-14.3	-13.9
90	33	28.2	25.5
100	-23.8	-15.4	-14.6
120	-34	-25.5	-25
140	-38.7	-29	-28.5
160	-42.9	-34.4	-35
180	-52	-44	-46

4. CONCLUSION

The electric field integral equation (EFIE) has been used with the Method of Moment (MoM) to develop a simple and efficient numerical procedure for treating problems of radar cross section (RCS) prediction of regular shaped objects. For numerical purposes, the objects were modeled using planar triangular surfaces patches. Because the EFIE formulation is used, the procedure is applicable to both open and closed surfaces. Crucial to the numerical formulation is the development of a set of special sub-domain-type basis functions, which were defined on pairs of adjacent triangular patches and yield a current representation free of line or point charges at sub-domain boundaries. A dipole model approach was used to calculate the scattering field in free space from the calculated current values. The two main advantages of integral equation methods for large exterior scattering problems are the reduction in dimensionality of the problem, and the ability to model infinite domains accurately. These must be weighed against the increased complexity (over differential methods) in the formulation and their being less well suited for highly inhomogeneous problems.

REFERENCES

- [1] Johnson J.H. Wang, "Generalized Moment Methods in Electromagnetics – Formulation and computer solution of

- Integral Equation*”, John Wiley & Sons, Inc, New York, 1991.
- [2] E.F. Knott, J.F. Shaffer and M.T. Tuley, “*Radar Cross Section*”, 2nd Edition, Artech House Radar Library, 1993.
- [3] H. Newman and D.M. Pozar, “Electromagnetic modeling of composite wire and surface geometries”, *IEEE Transactions on Antennas and Propagation*, Vol. 26, No. 6, pp. 784-789, 1978.
- [4] J.H. Richmond, “A wire-grid model for scattering by conducting bodies”, *IEEE Transactions on Antenna and Propagation*, Vol. 14, No. 6, pp. 782-786, 1966.
- [5] K.S.H. Lee, L. Marin and J.P. Castillo, “Limitations of wire-grid modeling of a closed surface”, *IEEE Transactions on Electromagnetic Compatibility*, Vol. EMC-18, No. 3, pp. 123-129, 1976.
- [6] Yau Lin and Richmond J, “EM modeling of Aircraft at Low Frequencies”, *IEEE Transactions on Antenna and Propagation*, Vol. 23, No. 1, pp. 53-56, 1975.
- [7] S.M. Rao, D.R. Wilton, and A.W. Glisson, “Electromagnetic scattering by surfaces of arbitrary shape”, *IEEE Transactions on Antenna and Propagation*, Vol. 30, No. 3, pp. 409-418, 1982.
- [8] Virga K.L and Rahmat-Sami Y, “RCS characterization of a finite ground plane with perforated apertures: simulations and measurements”, *IEEE Transactions on Antennas and wave propagation*, Vol. 42, No. 11, pp. 1491-1501, 1994.
- [9] Sidhu J.S, Kuster E.J, Friederich P.G and Hopkins E.J, “RCS prediction comparison between physical optics and moment method techniques”, *IEEE International symposium on Antenna and Propagation Society*, Vol. 2, pp. 1148 – 1151, 1997.
- [10] Do-Hoon Kwon, Robert J. Burkholder and Prabhakar H. Pathak, “Efficient Method of Moments Formulation for Large PEC Scattering Problems Using Asymptotic Phase front Extraction (APE)”, *IEEE Transactions on Antennas and Wave Propagation*, Vol. 49, No. 4, pp. 583-591, 2001.
- [11] X. F. Li, Y. J. Xie, and R. Yang, 2009, “Bistatic RCS prediction for complex targets using Modified Current Marching Technique”, *Progress In Electromagnetics Research*, Vol. 93, pp. 13–28, 2009.
- [12] Gonca Ç Akir and Levent Sevg, “Radar cross-section (RCS) analysis of high frequency surface wave radar targets”, *Turkish Journal of Electrical Engineering and Computer Sciences*, Vol. 18, No. 3, pp. 457-461, 2010.
- [13] C.A. Balanis, “*Antenna Theory: Analysis and Design*”, 2nd Edition, John Wiley & Sons, 1997.
- [14] Robert C Hansen, “*Moment Methods in Antenna and Scattering*”, Artech House Antenna Library, 1990.
- [15] Sergey. N. Makarov, “*Antenna and EM Modeling with MATLAB*”, Wiley-Interscience, 2002.